RESEARCH PAPER

PCCP
www.rsc.org/pccp

Heterogeneous interaction of Br_2, Cl_2 and Cl_2O with solid KBr and NaCl substrates: The role of adsorbed H_2O and halogens

Ch. Santschi and M. J. Rossi*

Laboratoire de Pollution Atmosphérique (LPA), Swiss Federal Institute of Technology (EPFL), CH-1015, Lausanne, Switzerland. E-mail: michel.rossi@epfl.ch

Received 23rd March 2004, Accepted 29th March 2004
First published as an Advance Article on the web 7th May 2004

The interaction of Br_2, Cl_2 and Cl_2O with different solid alkali halides, namely KBr and NaCl substrates, has been investigated in a low-pressure flow reactor. The observed main gaseous reaction products of the reactions of Cl_2 and Cl_2O with solid KBr substrates are Br_2 and BrCl. The reaction of Cl_2O with solid NaCl substrates leads to formation of Cl_2 and small amounts of HOCl. The role of surface-adsorbed H_2O (SAW) and the influence of adsorbed halogens have been investigated. Evidence for the formation of adsorbed Br_2 owing to mechanical stress has been found for solid KBr. Dehydration of the substrate under vacuum leads to a better ordered, more crystalline and hence less-reactive surface and decreases the number of reactive surface sites. Adsorption of halogen compounds such as BrCl, Cl_2 and Br_2 leads to effective dehydration of the KBr or NaCl substrate by competing for limited amounts of SAW. In this way, the reduced degree of hydration of the substrate alkali ions leads to activation of the halogen exchange reactions or catalytic activity.

Introduction

Studies on the decay of organics in marine air masses and sudden destruction of O_3 in the arctic troposphere[1–5] suggested the influence of halogen atoms that are formed by photodissociation of species such as Cl_2, Br_2, BrCl, HOCl, HOBr and others.[6,7] Atomic halogens are strong oxidizing species. As an example the oxidation rate of common gaseous hydrocarbons by atomic chlorine is approximately 100 times faster than by OH radicals.[8] The sudden ozone loss in arctic regions during polar sunrise cannot be explained by naturally occurring halogenated organics[9] such as methyl halides CH_3X or polyhalogenated species CHX_3 (bromo-, chloroform).[9,10] High chlorine concentrations measured in coastal air masses[8,11] suggest the existence of additional halogen sources such as marine salt aerosols MX (X = Cl, Br) generated by the action of wind and waves on the ocean's surface. Furthermore, a deficit of chlorine in marine aerosols compared to seawater has been found.[12] This chlorine deficit confirms the suggestion of marine aerosols as an important source of gaseous halogen species[10] that are released into the atmosphere by heterogeneous halogen exchange reactions[12,13] of HOY and $YONO_2$ (Y = Cl, Br) halogen reservoirs. These halogen activation reactions lead to the conversion of aerosol halide MX into volatile XY compounds releasing atomic halogens upon photolysis. Typical halogen activation reactions of salt aerosols may be described by reactions (1) and (2):

$$HOY + MX \rightarrow XY + MOH \ (X,\ Y = Cl,\ Br) \quad (1)$$

$$YONO_2 + MX \rightarrow XY + MNO_3 \quad (2)$$

Field studies have shown that free radical bromine is important in the photochemistry of the troposphere.[6,14] Bromine oxide, BrO, is proposed to be an important agent for tropospheric ozone depletion[2,15] during which BrO has been measured in concentrations of up to several tens of ppt.[16,17] Arctic field studies in the spring have shown an anticorrelation between BrO and a dramatic depletion of ground-level ozone on the time scale of one day or so,[2,6] the so called "bromine explosion" that occurs as the sunlight returns to the Arctic springtime.

The focus of the present work is placed on the fundamental study of the kinetics and mechanism of the heterogeneous interaction of chlorine and bromine containing compounds, namely Cl_2, Br_2 and Cl_2O, with solid alkali halide model substrates such as KBr and NaCl grains and thin films that mimick solid marine aerosol at low relative humidity corresponding to aerosol below its deliquescence point. Most of the experiments have been carried out in a low-pressure flow reactor in order to measure the reaction kinetics and determine the reaction products with an eye towards atmospheric applications. With the goal of a better understanding of the interaction mechanism, the role of surface adsorbed water (SAW) has been especially highlighted in this work. Understanding the role that SAW plays in heterogeneous reactions on salt enables bridging the gap between laboratory studies and atmospheric observations. An example of the importance of SAW is the intensely investigated reaction of HNO_3 on solid NaCl[18–21] where it enhances the mobility of interfacial ions in order to facilitate crystallization. In contrast, the rate of the same reaction on the (100) face of single crystal NaCl is slow under UHV conditions where there is no detectable amount of SAW.[22] Furthermore, it has been found that hydration of surface ions weakens ionic bond strengths[23] which may considerably change the chemical reactivity of the gas–solid interfaces. It also has been found that the adsorption of water on NaCl is correlated to the defect structure of the surface.[24] Surfaces of salt aerosols are far from being structurally perfect. Therefore, different sample presentations such as salt grains, ground grains and thin films have been used as model substrates in the present work. In summary, there is increasing evidence that H_2O adsorbed on defects on the substrate surface plays a key role in the reactivity of salt in halogen exchange reactions leading to the volatilization (= activation) of inorganic halide in the form of active halogen. Water preferentially adsorbs on crystal defects whose volume then becomes the controlling factor in the heterogeneous reactivity on salts.[25,33,39] However, the foregoing discussion on the quantity of SAW and its role as enabling factor in supporting ionic halogen exchange reactions will be much less important under atmospheric conditions at relative humidities exceeding the deliquescence point

DOI: 10.1039/b404415k

as atmospheric aerosols will exist in the form of concentrated salt solutions.

The companion paper, which deals with the reaction of HOCl with solid alkali halide model substrates,[26] is based on the results presented in this work.

Experimental

The uptake experiments have been performed in a low-pressure Teflon-coated Knudsen flow reactor. A detailed description of the apparatus is given by Caloz *et al.*[27] and the characteristic parameters of the Knudsen reactor used in the present work are presented in Table 1. The absolute concentrations of the reactants in the flow reactor range between 1×10^{10} and 5×10^{13} molecule cm^{-3} which corresponds to *ca.* 0.5 ppb–2 ppm at atmospheric pressure.

In this work two types of experiments are performed, namely steady-state (SS) and pulsed-valve (PV) experiments. A typical SS experiment involves introduction of a constant flow of the gaseous reactant through a capillary inlet into the reactor. A movable lid is used in order to isolate the sample against the gaseous reactant (lower position) or connect the sample compartment to the reactor (upper position) which allows the comparison of the outgoing flow F_{out} of the reactant in the absence and the presence of the solid sample. The details of these experiments are presented by Caloz *et al.*[27]

The corresponding uptake coefficient γ is defined according to eqn. (E1):

$$\gamma = \frac{k_{uni}}{\omega} \qquad \text{(E1)}$$

where k_{uni} is the first order rate constant for the uptake reaction and ω the collision frequency with regard to the whole sample surface. The uptake coefficient γ describes the reaction probability per collision.

In a PV experiment, the gas is injected into the flow reactor through a solenoid valve. The pulse lengths are typically in the range of a few hundreds of microseconds to ten milliseconds leading to doses between 10^{12} and 10^{16} molecule pulse^{-1}. When the sample compartment is closed, the reactant decay of the MS-signal corresponds to the effusion rate constant k_{esc}. A pulse fired into the reactor with the closed sample compartment is a reference pulse. The reactive pulse is obtained by admitting an identical dose with the sample exposed to the flow. The decay of this MS-signal is given by k_{dec} and corresponds to the sum of k_{uni} and k_{esc} according to eqn. (E2).

$$k_{dec} = k_{uni} + k_{esc} \qquad \text{(E2)}$$

Table 1 Knudsen flow reactor parameters

Parameter		Value
Reactor volume/cm^3		1830
Estimated surface area/cm^2		1300
Sample compartment surface area/cm^2		19.6
Chopper frequency/Hz		70
Orifice-Ø/mm		1, 4, 8 and 14
Collision frequency $\omega = \sqrt{\frac{8RT}{\pi M}} A_s/4V$		$39\sqrt{\frac{T}{M}}$ [a]
Escape rate constant k_{esc} [b]:	1 mm orifice	0.01 $(TM^{-1})^{\frac{1}{2}}$s^{-1}
	4 mm orifice	0.24 $(TM^{-1})^{\frac{1}{2}}$s^{-1}
	8 mm orifice	0.79 $(TM^{-1})^{\frac{1}{2}}$s^{-1}
	14 mm orifice	1.77 $(TM^{-1})^{\frac{1}{2}}$s^{-1}

[a] ω calculated for the geometric area of the sample [b] experimentally determined values. T and M are temperature and molar mass, respectively. $[T] = \text{K}$, $[M] = \text{g mol}^{-1}$

Thus, the uptake coefficient, γ, is given by eqn. (E3).

$$\gamma = \frac{k_{dec} - k_{esc}}{\omega} \qquad \text{(E3)}$$

The advantages of real-time pulsed valve experiments are:

(1) Exposure of the solid sample to small doses, of the order of a few percent of a surface monolayer, leading to small extents of surface saturation.

(2) Observation of the rate of product formation at high time resolution. This may be useful for studies of the reaction mechanism.

(3) Straightforward check of mass balances supporting a given reaction mechanism.

Gaseous samples

In order to remove residual HCl from commercially available Cl_2 it was pumped through NaOH pellets, thereby making use of the very exothermic reaction (3):

$$NaOH + HCl \rightarrow NaCl + H_2O \qquad (3)$$

Cl_2 was monitored using the mass spectrometer at the parent peak m/z 70 (100%) and m/z 35 (33%), where the value in the brackets indicates the relative intensity with respect to the base peak.

In order to remove residual H_2O from commercially available Br_2 it was pumped through P_2O_5 before being used for synthetic purposes. Br_2 has been monitored at the base peak m/z 160 (100%) but also at m/z 79 (25%) and m/z 81 (25%).[28]

Preparation of Cl_2O

Dichloromonoxide, Cl_2O, has been synthesized by reacting Cl_2 with solid mercuric oxide, HgO,[29] according to reaction (4):

$$2Cl_2 + 3HgO \rightarrow HgCl_2 \cdot 2HgO + Cl_2O \qquad (4)$$

The reacting mixture of HgO–Cl_2 has been kept at least 24 h in a circulating methanol bath at $T = 193$ K in order to complete the reaction. The separation of excess Cl_2 from Cl_2O has been performed by distillation in a standard vacuum line. The Cl_2 has been pumped off at $T = 200$ K from the mixture of Cl_2O and Cl_2, which has been monitored by mass spectrometry at m/z 51 and 70, respectively. The contribution to m/z 51 is 5% of m/z 52 for HOCl. Cl_2 could almost completely be removed from the sample. The purified Cl_2O was stored in a methanol cooling bath at $T = 190$ K for long-term storage. Pure Cl_2O is an explosive at ambient temperature and has to be handled with due care.[30]

Solid samples

Commercially available KBr and NaCl (Fluka AG) whose purity exceeded 99.5% have been used as solid substrates in uptake experiments of gaseous halogen species described in this work. The major impurities in KBr are chloride (Cl) ≤ 1000 mg kg^{-1}, sodium (Na) ≤ 200 mg kg^{-1} and sulfate (SO_4) ≤ 50 mg kg^{-1}. The impurities in NaCl are sulfate (SO_4) ≤ 100 mg kg^{-1}, bromide (Br) ≤ 50 mg kg^{-1}, iodide (I) and calcium (Ca) ≤ 10 mg kg^{-1}.

Grain samples

In this work, commercially available polycrystalline KBr and NaCl salts are called standard grains. The diameter d of the KBr and NaCl grains has been determined by optical microscopy to be of the order of $d = 150$ μm and $d = 400$ μm, respectively. The ratio between the apparent density of KBr grains to bulk crystalline KBr has been measured as $\frac{\rho_g}{\rho_c} = 0.47$ from the weight of KBr grains filled into a known volume V resulting in an apparent density $\rho_g = 1.3$ g cm^{-3}

compared to $\rho_c = 2.75$ g cm^{-3} for crystalline KBr.[30] For NaCl we obtained $\frac{\rho_g}{\rho_c} = 0.65$, with $\rho_g = 1.4$ g cm^{-3} and $\rho_c = 2.17$ g cm^{-3}.[30] The sample mass has been measured using a balance Mettler Toledo model PR5002 DeltaRange.

The total external surface area A_S of the KBr and NaCl grains is of the order of 145 cm^2 g^{-1} and 69 cm^2 g^{-1}, respectively, which was calculated from the apparent density and the average size of the grains knowing that salt is non-porous (Table 2).[31] The surface area A_S per gram of sample has been calculated using a cubic approximation for the grains according to eqn. (E4):[32]

$$A_s = 6\frac{1}{\rho_c d} \qquad \text{(E4)}$$

The BET surface of KBr of comparable particle size (125–200 μm) measured by Walter[33] is $A_{BET} = 440$ cm^2 g^{-1} and is higher than the surface A_s (Table 2) calculated from the dimension of the salt grains from eqn. (E4). This may be due to the uncertainty of the particle size d and the applied cubic approximation.

The surface number density n_S of the salt sample corresponding to the number of ion-pairs cm^{-2} has been approximated as follows:[34]

$$n_s = \sqrt[\frac{2}{3}]{\frac{\rho_c}{M_A} N_A} \qquad \text{(E5)}$$

where M_A is the molecular weight and N_A Avogadro's number. The calculated surface number densities n_S are listed in Table 2.

The total number of superficial ion-pairs results in $N = 8.4 \times 10^{16}$ and 5.4×10^{16} ion-pairs g^{-1} for KBr and NaCl, respectively, using eqns. (E4) and (E5).

Ground grain samples

Commercially available salt grains have been crushed by hand using a pestle and mortar. The particle size has been determined by optical microscopy to be of the order of 10 μm. The ratio $\frac{\rho_{gg}}{\rho_c}$ between the density of ground and crystalline KBr grains is 0.55 with $\rho_{gg} = 1.5$ g cm^{-3}. The density ρ_{gg} of ground KBr has been determined in the same way as for KBr grains.

The total external surface area A_S of ground KBr grains has been estimated using eqn. (E4) and is 2200 cm^2 g^{-1}. For ground KBr grains, the total number of superficial ion-pairs is 1.3×10^{18} molecule g^{-1} using eqns. (E4) and (E5) and is listed in Table 2.

Thin salt films deposited on a Pyrex sample holder

Commercially available salt grains have been dissolved in pure methanol (Fluka AG, purity $\geq$ 99.8%) whose saturated salt solution has been sprayed onto a Pyrex glass plate of 19.6 cm^2 cross section heated up to $T = 500$ K. The spray has been dispensed using an ESBE type atomizer from Thayer & Chandler powered with gaseous N_2. The solvent immediately evaporates over the hot Pyrex plate and the salt forms a coherent film across the substrate of the Pyrex support when the sample has been slowly cooled down to ambient temperature. The homogeneity of the salt coverage has been checked by means of scanning electron microscopy (SEM) (to be discussed below).

Table 2 Sample parameters of KBr and NaCl

	KBr g/gg[a]	NaCl[b]
ρ_c/g cm^{-3} [30]	2.75	2.17
M_A/g mol^{-1} [56]	119	58.4
n_s/molecule cm^{-2}	5.8×10^{14}	7.9×10^{14}
A_S/cm^2 g^{-1} [c]	145/2200	69
N/molecule	$8.4 \times 10^{16}/1.3 \times 10^{18}$	5.4×10^{16}

[a] g and gg are KBr standard and ground grains, respectively. [b] NaCl standard grains. [c] Calculated values.

A typical mass m of a salt film is of the order of 5 to 10 mg that corresponds to a thickness h between 1 and 2 μm. The weight measurements have been performed using a Mettler Toledo balance model AE 240. The thickness h has been calculated using the true density of crystalline KBr ρ_c and the geometric area A_g of the Pyrex support.

$$h = \frac{m}{\rho_c A_g} \qquad \text{(E6)}$$

Films prepared using H_2O–methanol–salt solutions have also been used for uptake experiments. Solutions that contain more than 10% v/v of H_2O have not resulted in homogeneous salt film coverage. While spraying the H_2O–methanol–salt solution across the hot Pyrex sample holder small particles of KBr have been formed and blown away by the jet of the atomizer as the KBr particles did not adhere to the Pyrex plate.

Thin KBr salt films on a gold-plated sample holder

Thin salt films deposited on a gold-plated support have been prepared in the same way as those on the Pyrex sample holder. In contrast to the thin KBr films sprayed on a Pyrex sample holder the temperature T of the gold-plated sample holder was set at $T = 350$ K and the N_2 flow had to be reduced considerably for better adhesion of the salt–methanol solution. The homogeneity of the thin salt film prepared as described, was checked using SEM.

Results and discussion

A. Surface-adsorbed H_2O (SAW)

In order to estimate the amount of surface adsorbed water (SAW[19]) desorption experiments have been performed in the low-pressure flow reactor. For this purpose, the KBr samples have been pumped for a given time before they have been heated in the flow reactor in order to probe for the remaining SAW by desorption. In order to point out the presence of strongly- and weakly-bound SAW the samples have been heated at first to a temperature of $T = 400$ K. Once the MS-signal of H_2O returned to the background level the temperature has been increased to $T = 620$ K in order to desorb strongly-bound SAW. Fig. 1 shows that weakly-bound SAW

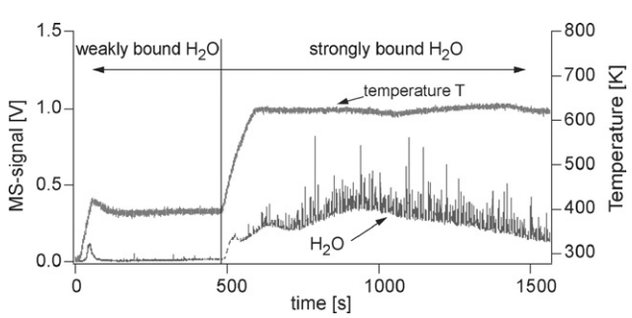

Fig. 1 Desorption experiment carried out on KBr grains in the 14 mm-orifice reactor. H_2O has been monitored at m/z 18. In order to demonstrate the presence of weakly- and strongly-bound SAW it has been desorbed at $T = 400$ K and 620 K, respectively. The spikes of the MS-signal at higher temperature correspond to small bursts of H_2O vapour which is enclosed in the KBr grains.

makes up at most 5% of the total SAW. At temperatures higher than approximately $T = 600$ K thermal emission of small quantities of K^+ may slowly set in.[35,36] The reference experiment with the bare gold-coated sample has shown a negligible amount of SAW desorbing from the internal walls of the flow reactor including the empty sample support.

Figs. 1 and 2 show the MS-signal of a desorption experiment carried out in the 14 mm-orifice reactor and the total amount of SAW probed as a function of the pumping time t_p, respectively. An extrapolation to large desorption times using an exponential fitting to the data of Figs. 1 and 2 has shown that the displayed data missed at most 15% of the total amount of SAW. However, the low SAW regime is not of primary interest in the present work. These experiments have been performed on KBr grains, ground grains and thin sprayed films that were all supported on a gold-coated sample holder. The obtained desorption-time curves have been used for other uptake experiments in order to convert pumping time t_p into an estimated number of SAW molecules still remaining on the substrate after t_p. A reference desorption experiment using a bare Pyrex plate has revealed that the amount of SAW on the Pyrex plate is many times higher than the SAW on the thin KBr film sprayed onto a Pyrex sample holder. This makes the determination of the amount of SAW on Pyrex supports virtually impossible. The amount of SAW under ambient conditions (at $t = 0$) may not be measured using this method because the sample needs to be pumped for several minutes in order to reach molecular flow conditions.

Scanning electron microscopy (SEM) has been used in order to investigate the influence of SAW on the morphology of the substrate. A thin film of KBr sprayed on a gold-coated sample holder exposed to ambient conditions has been compared with a substrate prepared in the same way but that has been heated under vacuum conditions to $T = 620$ K. Figs. 3a and 3b display SEM-images which show that heating leads to irreversible crystallization of the KBr substrate. Irreversible means that even under ambient conditions the crystalline sample does not convert towards a structure shown in Fig. 3a. For NaCl, Harrison *et al.*[37,38] have shown that bulk diffusion appears to start at a temperature far below the melting point T_m. In analogy to NaCl we conclude for KBr that bulk diffusion will lead to structural change of the surface even at temperatures much below the melting point of $T_m(KBr) = 1007$ K.[30] Furthermore, we have evidence from SEM that not only bulk diffusion but also dehydration of the substrate may enhance the rate of crystallization (reaction (5)).

$$K\text{–}Br(H_2O)_n \rightarrow KBr(c) + nH_2O \qquad (5)$$

By hydration we mean an incipient dissolution process in H_2O. Within the bounds of our experiments, we may not distinguish between contact, solvent-separated and totally dissolved ion-pairs. Similar behavior has been observed on $Ca(NO_3)_2$ particles in the presence of SAW.[39] Tang and Fung found that $Ca(NO_3)_2$ forms amorphous metastable states in hygroscopic microparticles. The presence of SAW is a prerequisite for the formation of the amorphous states. After complete removal of the adsorbed water an anhydrous crystalline particle forms which underlines the role that SAW plays to enable the mobility of ions in the formation of a crystalline phase.

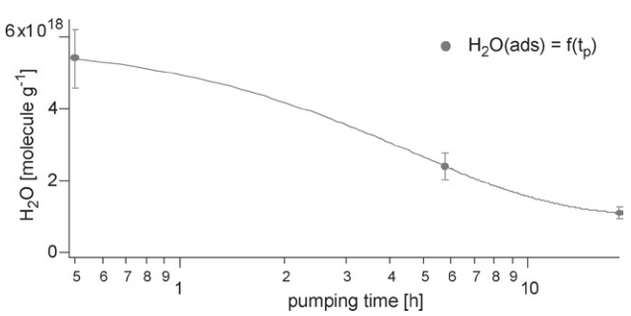

Fig. 2 Quantity of the total amount of SAW on KBr grains as a function of pumping time t_p. The sample has been pumped for a given time t_p within the Knudsen flow reactor to $p = 10^{-6}$ Torr before the residual SAW has been desorbed by heating the sample to $T = 620$ K.

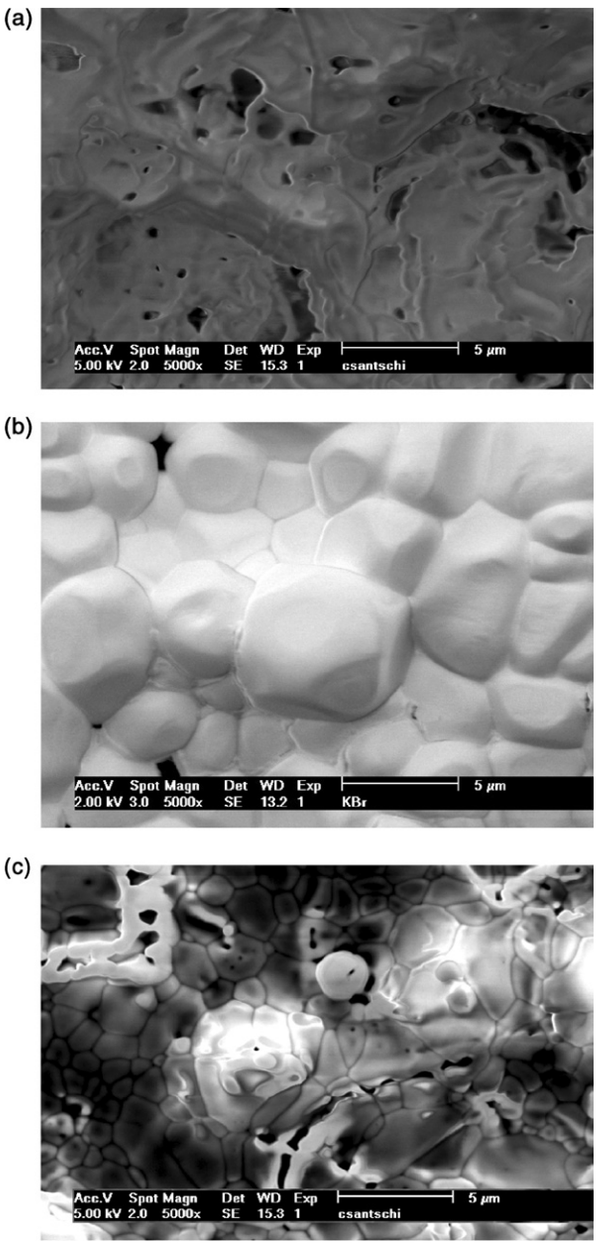

Fig. 3 (a) SEM-image of a thin KBr film sprayed a on gold-coated copper sample holder. The sample has been exposed for four days to atmospheric conditions. (b) SEM-image of a thin KBr film sprayed on a gold-coated copper sample holder. The sample has been heated to $T = 620$ K *in situ*. (c) SEM-image of a thin KBr film sprayed on a gold-coated copper sample holder. The sample has been pumped $p = 10^{-6}$ Torr in the 14 mm-orifice reactor for four days.

SEM-images of thin KBr films sprayed on gold-coated sample holders that have been dehydrated by pumping to an ultimate partial pressure of H_2O of 10^{-6} Torr are displayed in Fig. 3c. A comparison of Fig. 3c with Fig. 3a reveals a change towards a better-ordered surface. Using atomic force microscopy (AFM) Dai[23] observed that by lowering the humidity over a NaCl substrate relatively well-ordered surfaces may be obtained which is in qualitative agreement with our observation on thin KBr films sprayed on a gold-coated sample holder. The change of the substrate

is irreversible which is a hint for the presence of different types of surface sites, namely hydrated K–Br$(H_2O)_n$ and more stable KBr(c) that do not all revert to hydrated K–Br$(H_2O)_n$ at ambient conditions.

During the heating of KBr grains, ground grains as well as thin KBr film sprayed on a gold-coated copper sample holder we have monitored HBr, HOBr and Br_2 at m/z 82, m/z 96 and m/z 160, respectively. HBr has only been observed in small amounts, whereas desorption of HOBr has been observed on KBr ground grains and thin KBr films sprayed on a gold-coated copper sample holder as displayed in Fig. 4. In contrast to the above mentioned samples, no desorption of HOBr has been observed on KBr grains under similar conditions. No desorption of Br_2 has been observed on any of the investigated substrates.

The desorption of HBr may be due to the hydrolysis of KBr according to equilibrium (6a) which is in analogy to equilibrium (6b) for NaCl,[40] the reverse of the very exothermic acid–base titration reaction:

$$\mathrm{KBr(s) + SAW \rightleftarrows K{-}OH + H{-}Br} \qquad (6a)$$

$$\mathrm{NaCl(s) + SAW \rightleftarrows Na{-}OH + H{-}Cl} \qquad (6b)$$

Desorption of HOBr is a one-time event that has only been observed for a sample that has been heated for the first time at a temperature above $T = 470$ K. Subsequent heating of the same sample has not led to additional desorption of HOBr. Bulk KBr does not decompose at $T = 620$ K,[35] whereas specific surface sites of KBr obviously lead to the release of HOBr and HBr which must be associated with the presence of SAW and the defect surface structure of the substrate. At this point, one is reminded that KBr grains do not release HOBr in contrast to ground grains and thin solid films.

The formation of HOBr has to be accompanied by a change of the oxidation state of bromine in KBr. Together with the strongly endothermic reaction (7) the present result leads us to the postulate of the presence of hydrated adsorbed molecular Br–Br which decays to HOBr and HBr while the sample is heated to $T = 620$ K in the presence of SAW.

$$\mathrm{Br - Br + SAW \overset{Q}{\rightleftharpoons} HOBr + HBr} \qquad (7)$$

The presence of adsorbed Br–Br, perhaps in the form of an ion pair Br^+Br^-, may be the chemical indicator for the formation of a F-center or other active site within the alkali halide substrate. By grinding the KBr grains an anion may be pulled out of the crystal matrix owing to local mechanical stress including evaporation of the aqueous solvent thereby leaving a vacancy where an electron e^- may be trapped.[41] V_k centers of the type $[Cl\cdots NO_2]^-$ or $[Br\cdots NO_2]^-$ have been observed resulting from the reaction of NO_2 with ground NaCl and NaBr, respectively.[42] Reaction (8) may describe a possible charge exchange process leading to adsorbed molecular bromine which may undergo a disproportionation reaction upon heating following reaction (7). Owing to the small concentrations and/or rapid reaction of adsorbed Br_2, such as reaction (7), none was observed to desorb to be detected.

$$\mathrm{2K^+Br^- \xrightarrow{mechanical\ stress} 2K^+ + Br - Br + 2e^-} \qquad (8)$$

Reaction (8) represents a charge-exchange or internal redox process that apparently does not occur on standard KBr grains. Therefore, we rule out an oxidizing impurity in the KBR sample. Infrared spectra of freshly ground KBr samples taken in an IR photoacoustic cell (MTEC Photoacoustics Model 300) manifest a more intense broad peak centered at 600 cm^{-1} than spectra of standard grains. However, upon exposing such a ground KBr grain sample to the ambient atmosphere for 24 h, the IR signature at 600 cm^{-1} decays away, thus showing that the surface of freshly ground grains is unstable under ambient conditions.

In order to check the surface for basic OH-sites formed by equilibrium (6a), KBr grains have been exposed to CO_2. Dai *et al.*[40] have shown for NaCl using FTIR-spectroscopy that the formation of basic sites through equilibrium (6b) occurs on defect sites. Uptake of CO_2 on KBr grains may be an indicator for surface OH-sites in analogy to the reaction with NaOH[38] according to reaction (9).

$$\mathrm{Na{-}OH(s) + CO_2(g) \rightleftarrows Na^+(HCO_3)^-} \qquad (9)$$

We assume that CO_2 interacts with OH-sites formed on the KBr surface according to equilibrium (6) in the presence of SAW because it is not known that CO_2 reacts with bulk NaCl.[43] Therefore, we assume that CO_2 does not directly interact with KBr, instead we propose that a reaction with OH-sites on solid KBr occurs according to reaction (10) in analogy to reaction (9):

$$\mathrm{K{-}OH(s) + CO_2(g) \rightleftarrows K^+(HCO_3)^-} \qquad (10)$$

The total loss of CO_2 is measured to be 7×10^{14} molecule g^{-1}. Use of the estimated surface area $A_S = 145 \times 10^{-4}$ m^2 g^{-1} leads to a loss of CO_2 of 1×10^{12} molecule cm^{-2}. Comparing with the calculated KBr surface density of ion pairs of 5.8×10^{14} molecule cm^{-2} (Table 2) we conclude that the surface of KBr grains contains basic sites which may react with CO_2 corresponding to less than 1% of the total surface area. This number is comparable to the results of Ewing and coworkers on NaCl.[40]

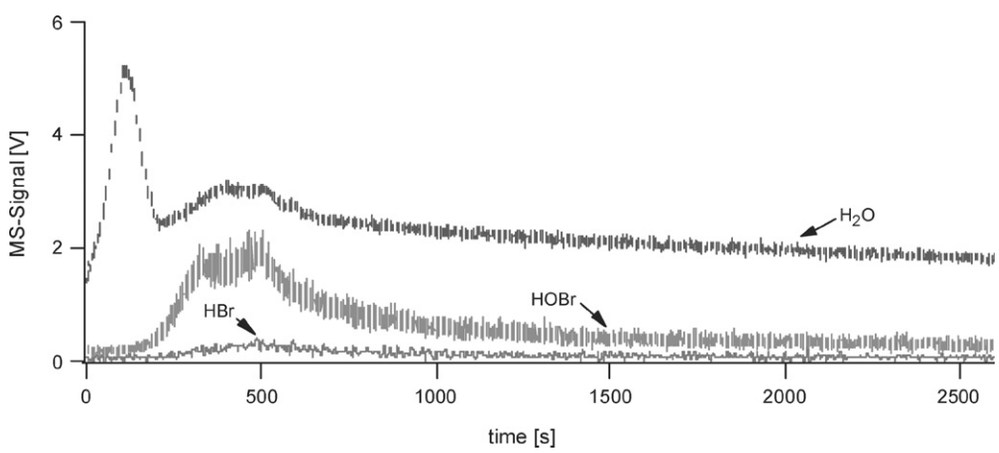

Fig. 4 MS-signal of H_2O, HOBr and HBr desorbing from a thin film of KBr sprayed on a gold-coated copper sample holder carried out in the 14 mm-orifice reactor at temperature $T = 620 \pm 2.5$ K. The signal of H_2O has been recorded at 10 times smaller sensitivity compared to HBr and HOBr.

In this section, we have presented desorption experiments in order to estimate the amount of SAW. Furthermore, we have proposed the presence of molecular and hydrated Br–Br pairs described by Br^+–Br^- on ground KBr grains and thin KBr films sprayed on a gold coated sample holder, as well as the presence of basic OH-sites generated by hydrolysis of KBr by SAW according to reaction (6). The hyphen represents a hydrated ion-pair.

B. Interaction of Br_2 with KBr

A net Br_2 uptake on solid KBr samples, that is a non-reactive uptake at ambient temperature, has never been observed under the conditions of low-pressure flow reactor steady-state experiments. Nevertheless, while performing pulsed valve experiments of Br_2 on solid KBr substrates an interaction leading to an uptake coefficient of $\gamma = 3 \times 10^{-3}$ has been observed.[44]

In order to demonstrate the interaction of Br_2 with KBr, thin films sprayed onto a Pyrex support have been exposed in a static reactor to 50 mbar of Br_2 after they had been pumped for 1 h in a standard vacuum line at ambient temperature to a total pressure lower than 1 mbar. After two days of Br_2 exposure, SEM images of a sample exposed to Br_2 and one exposed to ambient conditions have been taken. Figs. 5a and 5b show a sample exposed to ambient conditions and one exposed to Br_2, respectively.

The interaction of Br_2 with thin films of KBr manifests itself in the crystallization of KBr, whereas the sample exposed to ambient conditions did not show a noticeable change towards a more ordered surface when exposed for the same length of time. The observed surface change upon Br_2 exposure is irreversible which means that the exposure of the well-ordered sample to ambient conditions does not lead back to a lower-ordered surface.

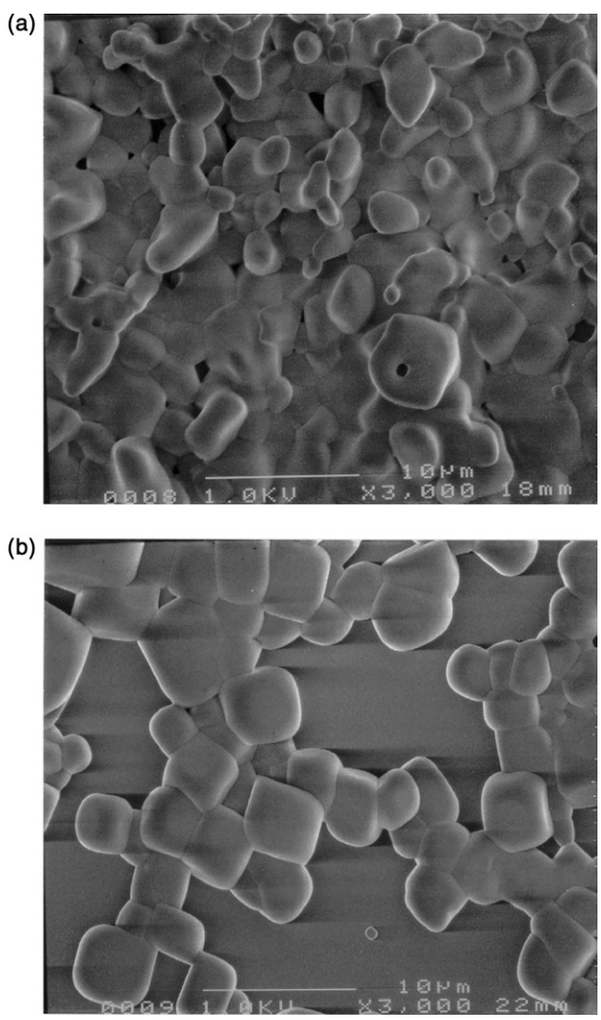

Fig. 5 (a) SEM image of a thin KBr film sprayed on Pyrex sample holder exposed for 2 days to ambient conditions. (b) SEM image of a thin KBr film sprayed on Pyrex sample holder exposed for 2 days to 50 mbar of Br_2.

As mentioned above, hydrated KBr is thermodynamically less stable than the crystalline form as shown by the following values: $\Delta H_f^0 + -393.8$ and -373.9 kJ mol^{-1} for hydrated and crystalline KBr,[45] respectively. The presence of adsorbed Br_2 seems to lower the energy-barrier between the less- and the higher-ordered state which is characterized by an increased rate of crystallization.

The observed crystallisation of the KBr films may be explained by the presence of a quasi-liquid layer (QLL) consisting of SAW[18] which interacts with Br_2. We propose the following reaction mechanism because Br_2 is obviously required for efficient crystallization of KBr:

$$\mathrm{KBr(s) + SAW \rightleftarrows K{-}OH(s) + H{-}Br(a)} \qquad (6)$$

$$\mathrm{Br_2 + SAW \rightleftarrows HO{-}Br(a) + H{-}Br(a)} \qquad (11)$$

$$\mathrm{K{-}OH(s) + H{-}Br(a) \rightarrow KBr(c) + SAW} \qquad (12)$$

We explain the efficient crystallization of KBr in the presence of Br_2 with two effects: first, adsorbed Br_2 acts as a dehydrating agent which leads to dehydration of the KBr surface under vacuum conditions (reaction (11)). A deficiency of SAW leads to crystallization of the surface, as we have shown in the previous section (reaction (5)). Second, the hydration of adsorbed Br_2 leads to an excess of mobile Br^- ions in the form of H–Br which may enhance the rate of the crystallization process of KBr (reaction (12)).

An unmistakable sign of the interaction of a gas with a solid substrate is the measurement of an observable surface-residence time τ_s of the gaseous species. To this end, the measurement of τ_s of Br_2 on KBr grains has been carried out in the low-pressure flow reactor in stopped-flow experiments. In order to detect Br_2 desorbing from the sample, the flow of Br_2 was suddenly turned off.

The surface residence time τ_s has been calculated using the following linear equation system:

$$\begin{pmatrix} \dot{N} \\ \dot{S} \end{pmatrix} = \begin{pmatrix} -(k_{esc} + k_a) & k_d \\ k_a & -k_d \end{pmatrix} \begin{pmatrix} N \\ S \end{pmatrix} \qquad (E7)$$

where N and S represent the number of Br_2 molecules in the volume of the reactor and on the surface, respectively, and k_a and k_d are the rate constants for adsorption and desorption, respectively. Solving eqn. (E7) leads to the following expressions for k_d and k_a:

$$k_d = \frac{\lambda_1 \lambda_2}{k_{esc}} \qquad (E8)$$

$$k_a = \frac{(\lambda_1 - k_{esc})(k_{esc} - \lambda_2)}{k_{esc}} \qquad (E9)$$

where $\lambda_{1,2}$ are the eigenvalues of the matrix given in eqn. (E7). The residence time, τ_s, is given by eqn. (E10):

$$\tau_s = \frac{1}{k_d} \qquad (E10)$$

with the residence time τ_c per collision given as follows:

$$\tau_c = \frac{\tau_s}{n_c} \qquad (E11)$$

with n_c (eqn. (E12)) being the average collision number of the molecule with the substrate surface during its residence in the reactor.

$$n_c = \frac{\omega}{k_{esc}} \qquad (E12)$$

Table 3 Eigenvalue and surface-residence time of Br_2 on 1 g of KBr grains at 300 K ($A_s = 145\ cm^2\ g^{-1}$)

Orifice/ mm	$[Br_2]$/molecule cm^{-3}	λ_1/s^{-1}	λ_2/s^{-1}	k_{esc}/s^{-1}	τ_s/s	τ_c/ms
4	1.2×10^{13}	0.16	0.29	0.28	6	4.3
14	1×10^{12}	1.25	2.3	2.4	0.8	5.1

In order to calculate the collision frequency ω, the surface area $A_s = 145\ cm^2\ g^{-1}$ obtained by the cubic approximation has been used.

The eigenvalues of the system have been determined by fitting the MS-signal of the stopped-flow experiments to a biexponential decay. The values for the 4 - and 14 mm-orifice reactor are listed in Table 3. The obtained surface residence time per collision τ_c is 4.7 ± 0.5 ms for KBr grains. This significant residence time suggests that adsorbed Br_2 may undergo reactions with other adsorbed or gaseous species which will be discussed in the context of uptake experiments of HOCl on KBr presented in a forthcoming paper.[26]

C. Uptake experiments of Cl_2 on KBr

In order to investigate the products of the reaction of Cl_2 with solid KBr a MS scan of the effluent of the reactor at a steady-state flow rate of Cl_2 in the absence and the presence of KBr grains has been performed. The MS-scan of Cl_2 in the absence of salt revealed a slight impurity of HCl. Fig. 6 shows both formation of Br_2 monitored at m/z 79, 81 and 158, 160, 162 and slow production of HBr measured at m/z 80 and 82 in the presence of solid KBr. Comparison of the loss of HCl with the yield of HBr resulted in a one to one correspondence. Therefore, we conclude that the observed gaseous HBr originates from the reaction of the impurity HCl with KBr grains.

Consecutive uptake experiments of Cl_2 on KBr standard grains have been performed in the 14 mm-orifice reactor at $[Cl_2] = 6 \times 10^{11}$ molecule cm^{-3}. The delay between the first and the second experiment was approximately 10 min. On a fresh sample, the initial uptake coefficient was $\gamma_0 = 0.24$, however, a subsequent uptake experiment of Cl_2 on an already exposed sample led to $\gamma_0 = 5 \times 10^{-2}$. Although γ_0 is lower for an already exposed KBr sample, it is larger than the value $\gamma_{ss} = 2 \times 10^{-2}$ at the end of the first uptake experiment. This means that under the present vacuum conditions, a partial regeneration of reactive surface sites is taking place. A series of Cl_2 uptake experiments have been performed as a function of the time delay t_r or regeneration time at $[Cl_2] = 3 \times 10^{11}$ molecule cm^{-3} in the 4 mm-orifice reactor whose results are displayed in Fig. 7.

The regeneration may be due to crystallization of the product KCl, which leads to a release of SAW, reaction (13), in analogy to the KBr, reaction (5). Crystallized KCl is thermodynamically more stable than KBr, according to the standard heat of formation: $\Delta H_f^0 = -436.74$ *vs.* -393.8 kJ mol^{-1}, respectively.[45] Therefore, we propose that KCl formed on the surface from the reaction of Cl_2 with KBr may crystallize and liberate occupied sites. Rearrangement of the surface through crystallization in the presence of H_2O vapour has also been observed after reaction of HNO_3 with NaCl.[18]

$$K\text{–}Cl(H_2O)_n \rightarrow KCl(c) + nH_2O \qquad (13)$$

We propose this rate-limiting crystallization process in analogy to the HNO_3/NaCl and N_2O_5/NaCl systems investigated by Hemminger and coworkers[18,46,47] who observed a crystallization of the NaCl substrate surface leading to the formation of small $NaNO_3$ crystallites.

Furthermore, molecular dynamics simulations of concentrated aqueous NaCl solutions suggest that adsorbed halogen species tend to form clusters[48] with SAW. This may lead to a deficit of SAW upon adsorption, resulting in dehydration of K–Cl. This means that adsorbed halogen species, such as Cl_2, may withdraw H_2O from the mobile K–Cl in order to satisfy its own needs of solvation and thus initiate a crystallization process similar to the pumping action discussed in the previous section (Figs. 3a and 3c). Similarly, Zangmeister and Pemberton[49] have shown for the HNO_3/NaCl system that adsorbed HNO_3(a) must compete for H_2O. For the Cl_2/KCl system this may be described by reaction (14):

$$K\text{–}Cl + X_2(a) \rightarrow KCl(c) + X_2(H_2O)_n(a) \quad X = Cl,\ Br \qquad (14)$$

where K–Cl corresponds to hydrated KCl expressed as $KCl(H_2O)_n$.

In order to investigate the observed surface-contamination by adsorbed chlorine species we have performed pulsed valve experiments. Fig. 8 shows the MS-signal of a typical pulsed-valve (PV) experiment of Cl_2 interacting with a thin KBr film sprayed on a Pyrex sample holder performed in the 14 mm-orifice reactor.

Subsequent identical Cl_2 pulses of 1.8×10^{13} molecules each were injected into the reactor corresponding to less than 1% of the total amount of KBr ion-pairs of the surface of a thin KBr film sprayed onto a Pyrex sample holder. We have alternately recorded the MS-signal of Cl_2 and Br_2 at m/z 70 and m/z 160 for successive pulses, respectively. For one pair of pulses, the ratio R between the yield of Br_2 and the loss of Cl_2, namely $R = \frac{N_{Br_2}}{\Delta N_{Cl_2}}$, has been determined and displayed as a function of the sum over all injected molecules whose total injected dose

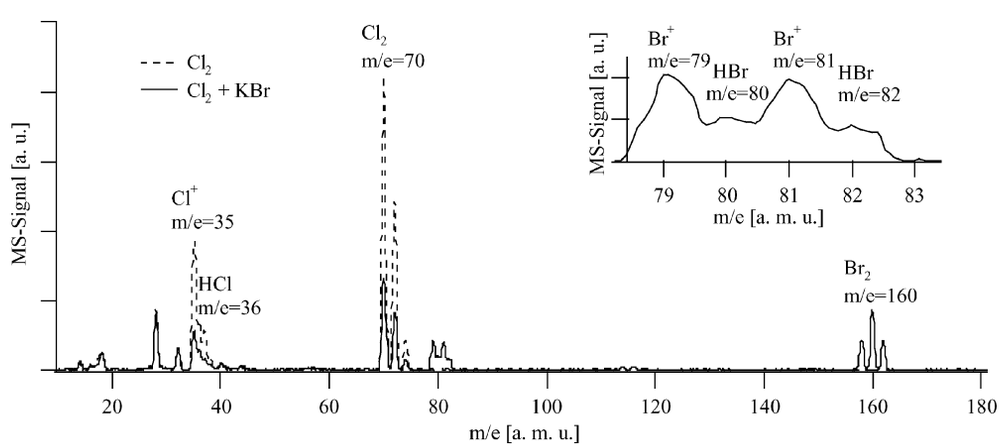

Fig. 6 Mass-spectrometric scan of the Cl_2 sample and the reaction of Cl_2 with KBr grains in the 4 mm-orifice reactor.

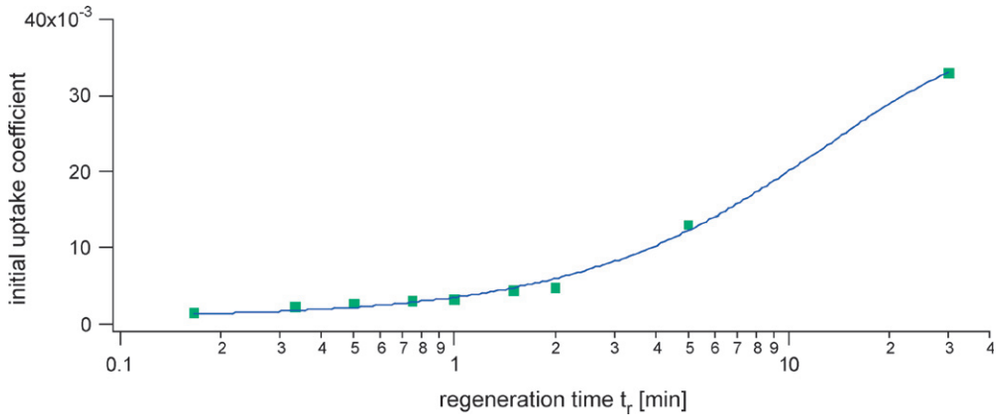

Fig. 7 Repetitive uptake experiment of Cl_2 on thin KBr film sprayed on a gold-coated copper sample holder carried out in the 4 mm-orifice reactor at $[Cl_2] = 5 \times 10^{11}$ molecule cm^{-3}. After reaching steady-state, the sample compartment has been isolated from the Cl_2 flow. After the regeneration time t_r, the sample had again been exposed to the same concentration of Cl_2.

is $D = K \sum \int^{\text{pulse}} S(t)\mathrm{d}t$, where K and $S(t)$ are the calibration factors for the MS-signal in molecule V^{-1} s^{-1} and the MS-signal for Cl_2 in V, respectively.

The PV experiments have shown absolute values of R less than 1 and an increase of R with increasing the number of pulses or equivalently with the total amount of the injected dose D of Cl_2 (Fig. 9a), which is an indication for surface contamination that is persisting from one pulse to the next. Knudsen cell uptake experiments of Cl_2 on NaCl and KCl carried out by Mochida[50] led to an uptake of Cl_2 but no products were observed, which confirms the suggestion of surface-adsorbed halogen. Galwey[51] has shown evidence of halogen retention on KBr surfaces based on the existence of polyhalide intermediates of the type $Cl_2Br^-K^+$ whose decay leads to formation of KCl. We suggest that these intermediates may be present on a poisoned surface leading to an increase of R and thus to enhanced formation of Br_2 with an increase of the total dose D of injected Cl_2, as is displayed in Fig. 9a.

In order to study the retention of halogens in more detail, experiments with different amounts of SAW have been performed. Thin films of KBr sprayed on a Pyrex sample holder have been pumped for different durations ranging from 15 min to 40 h which is a proxy for the amount of SAW remaining on the KBr sample. The R value for the sample pumped for 40 h is not significantly different from the briefly pumped sample. However, the effect on γ_0 is larger because prior pumping leads to a decrease of γ_0 from 0.15 to 0.04 for a sample pumped for 0.25 and 40 h, respectively. We explain this with the fact that dehydration of the surface according to reaction (5) leads to a loss of reactive sites due to a crystallization process that may also be viewed in Fig. 3c.

Further experiments addressed the effect of atmospheric exposure of a poisoned KBr substrate on R that has been exposed for 5 min to ambient conditions at $T = 293$ K and a relative humidity of 30% corresponding to approximately 6 Torr of H_2O. In contrast to the behaviour of the virgin KBr sample, the ratio R for the sample exposed to the ambient for 5 min and subsequently poisoned using an identical dose D of Cl_2 decreases with D, as displayed in Fig. 9b. Apparently, surface poisoning persists even under ambient conditions on the time scale of minutes.

In contrast to R, the corresponding γ values pertaining to results displayed in Figs. 9a and 9b are not significantly different if the virgin KBr thin film had been pumped for a while. This is consistent with the fact that the surface change, namely the induced crystallization owing to pumping is irreversible under ambient conditions, as has been shown in Figs. 3a and 3c.

The fact that γ does not significantly change after exposure to ambient conditions, as displayed in Table 4 whereas the yield of Br_2 increases after exposure to ambient H_2O

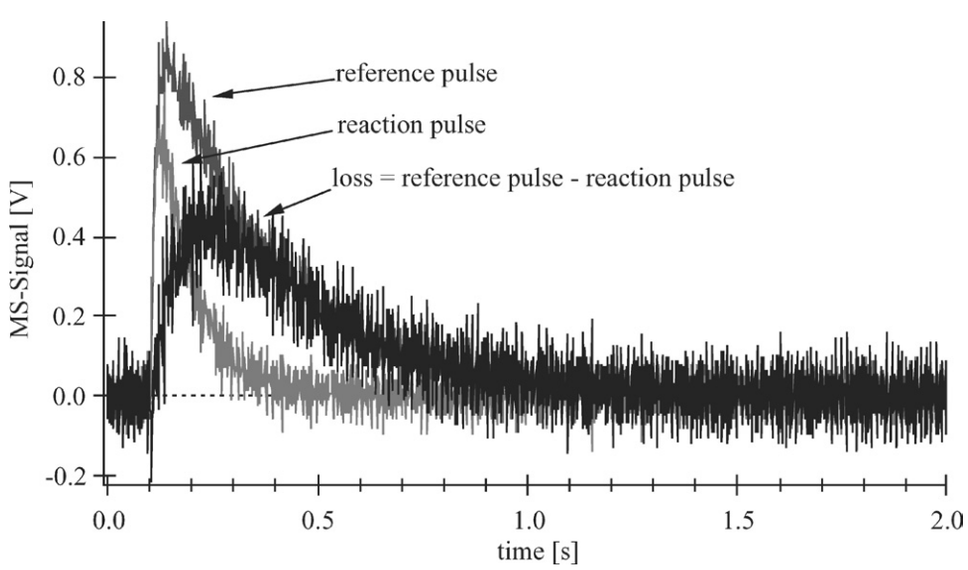

Fig. 8 Typical pulsed valve uptake experiment of Cl_2 on a thin film of KBr sprayed on a Pyrex support carried out in the 14 mm-orifice reactor. Cl_2 has been monitored at m/z 70. The opening time for Cl_2 dosing was $t_a = 1$ ms. The injection dose amounted to 1.8×10^{13} molecule $pulse^{-1}$.

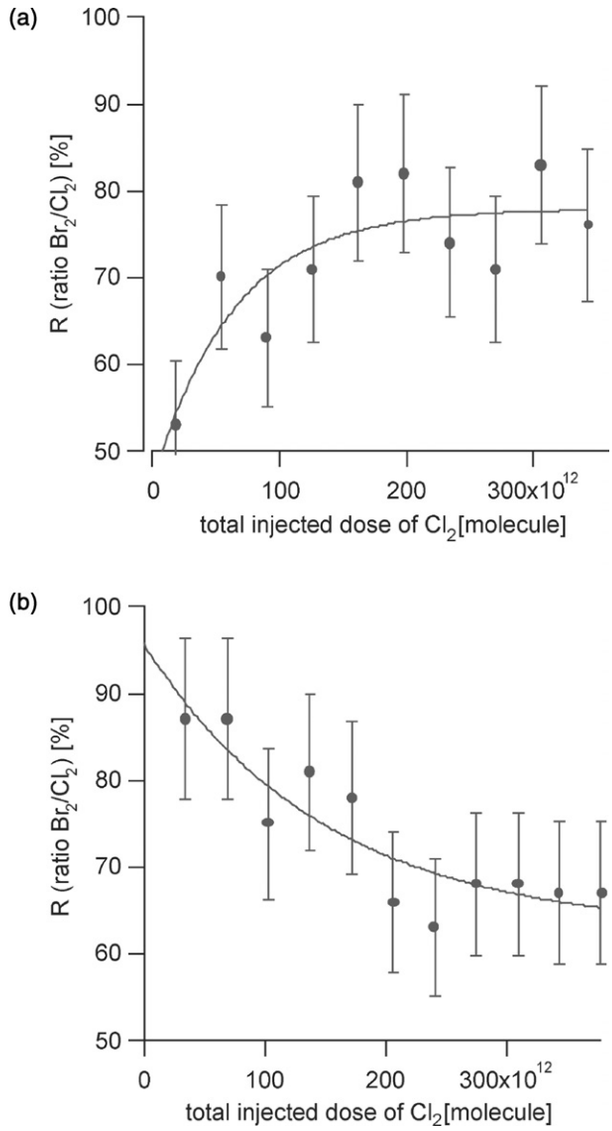

Fig. 9 Pulsed valve experiment of Cl_2 on a thin KBr film sprayed on a Pyrex sample holder performed in the 14 mm-orifice reactor. Part (a) shows the ratio $R = \frac{N_{Br_2}}{\Delta N_{Cl_2}}$ of an experiment carried out on a fresh and (b) on the same poisoned sample exposed to approximately 6 Torr of H_2O for 5 min and using the same Cl_2 dose.

(Fig. 9b) compared to the reference (Fig. 9a) leads to the following conclusions:

(i) The presence of SAW enhances the rate of conversion of surface adsorbed chlorine to surface-adsorbed bromine or polyhalide species such as Cl_2Br^-. This follows from the decrease of γ with removal of SAW by pumping, as shown in Fig. 2.

(ii) Adsorbed halogen or polyhalide species[51] is not removed from the surface during exposure to ambient conditions for several minutes. This follows from the large value of R after exposure of the poisoned sample to ambient conditions, as shown in Fig. 9b. Under these conditions, almost 100% of the lost Cl_2 may be converted into gaseous Br_2 after the first injection of Cl_2, in contrast to the *ca.* 50% conversion on a fresh KBr surface. Adsorbed halogen therefore catalyzes exchange reactions on solid KBr.

(iii) During the exposure of poisoned KBr to ambient conditions, the displacement of bromide by adsorbed chlorine continues to occur resulting in adsorbed Br–Cl or Br_2Cl^- and K–Cl, according to reactions (16) and (17). This explains the small change of γ after exposure to ambient conditions and a R value of almost 100% for the exposure of a KBr sample poisoned by Cl_2 to ambient conditions, as displayed in Fig. 9b.

These conclusions are consistent with the following proposed reaction scheme in which the expected primary reaction product BrCl does not desorb into the gas phase at low KCl coverage owing to the fast secondary reaction (17), in agreement with the efficient uptake of BrCl onto mixed, frozen salt surfaces,[52] that quickly consumes adsorbed BrCl leading to Br_2:

$$Cl_2 + S \rightleftarrows Cl_2\text{–}S \quad (15)$$

$$Cl_2\text{–}S + KBr \rightarrow BrCl\text{–}S + KCl \quad (16)$$

$$BrCl\text{–}S + KBr \rightarrow Br_2\text{–}S + KCl \quad (17)$$

$$Br_2\text{–}S \rightleftarrows Br_2 + S \quad (18)$$

$$\text{Net}: \quad Cl_2 + 2KBr \rightarrow Br_2 + 2KCl$$

The rapid rate of formation of Br_2 upon Cl_2 uptake on a spoiled KBr sample displayed in Fig. 9b may be explained by the displacement reaction (19). On a poisoned KBr sample exposed to ambient conditions adsorbed Br_2 may already be present so that reaction (19) just induces desorption by Cl_2.

$$Cl_2 + Br_2\text{–}S \rightarrow Cl_2\text{–}S + Br_2 \quad (19)$$

A precedent for such a mechanism has been discovered in the reaction of HNO_3 with NaCl or KBr.[53]

Fig. 10 shows a cartoon of the reaction mechanism given above. On a fresh KBr sample the interfacial halogen reservoir is filled up by adsorption of Cl_2 followed by reaction with reactive KBr-sites to form adsorbed BrCl(a), which interacts with a second KBr-site to form adsorbed molecular bromine (reactions (15)–(17)) (Fig. 10a). This leads to a small value of R because significant amounts of bromine are tied up in the surface reservoir. Between two subsequent pulses, the adsorbed chlorine may continue to react with adsorbed/dissolved bromine in the absence of gaseous Cl_2 (reactions (16) and (17), Fig. 10b). In the case of renewed exposure of the interfacial volume to Cl_2, an enhanced amount of bromine desorbs as a result of the displacement reaction (19) with Cl_2 (Fig. 10c). This leads to a large value of R. Case (a) in Fig. 10 corresponds to filling the SAW reservoir with Cl_2 whereas case (c) results in an enhanced rate of formation of Br_2 owing to the occurrence of reaction (19). These considerations led to the conclusions that the KBr substrate contains a double interface, namely zone 1 and zone 2, displayed in Fig. 10.

BrCl(g) was observed but its rate of formation and/or desorption sets in after a delay and increases with time whereas the rate of production of Br_2 decreases with time (Fig. 11). A

Table 4 Cl_2 pulsed valve experiments (first pulse) on thin KBr film sprayed on a Pyrex sample holder. The typical uncertainty in γ is of the order of 15%

No	Orifice diameter/mm	Cl_2/molecule pulse^{-1}	Experimental conditions	Main products	Uptake kinetics (first pulse)
1a	14	1.8×10^{13}	Pumping time $t_p = 40$ h	Br_2	$\gamma = 4 \times 10^{-2}$
1b	14	1.7×10^{13}	Exposure to 20 mbar H_2O, $t_{exp} = 5$ min	Br_2	$\gamma = 3.5 \times 10^{-2}$
2a	14	1.6×10^{13}	Pumping time $t_p = 0.25$ h	Br_2	$\gamma = 0.11$

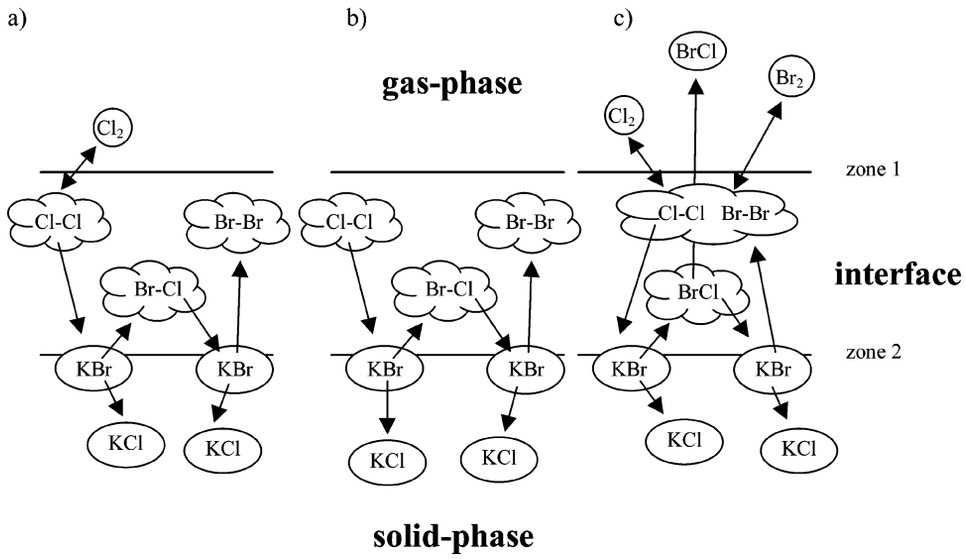

Fig. 10 Schematic illustration of the reaction of Cl_2 on KBr. Case (a) illustrates the reaction on a fresh sample. Cl_2 adsorbs in the interface region and is hydrated by SAW. The adsorbed Cl–Cl reacts with KBr at zone 2 which leads finally to a formation of Br–Br. Case (b) shows the reaction of adsorbed Cl–Cl in the absence of gaseous Cl_2. Adsorbed Cl–Cl leads to adsorbed Br–Br. Case (c) displays the reaction of Cl_2 on a poisoned sample. Gaseous Cl_2 displaces adsorbed Br–Br which is immediately, together with BrCl, released into the gas phase. The clouds indicate the adsorbed hydrated intermediate species.

delay of the formation of BrCl(g) has also been observed in the reaction of Cl_2 on NaBr[54] and is proposed to be the primary product.[55] The gradual increase of the rate of formation of BrCl(g) may be explained with the increasing surface coverage of KCl from a previous exposure of KBr to Cl_2, which consequently leads to a slower conversion of BrCl–S to Br_2 in reaction (17) owing to a lower number of reactive KBr sites. After an uptake of *ca.* 10 min, saturation sets in for the 1 mm-orifice reactor and the rate of production of Br_2 as well as BrCl tend to zero. Saturation means that only a fraction of the entire KBr sample is available to undergo reaction with Cl_2. This may be explained by the presence of a limited number of active surface-sites that increasingly may be poisoned under vacuum conditions by the build-up of non-reactive KCl.

In order to investigate the influence of adsorbed SAW on the reactivity, the standard KBr grains have been heated in an oven for 20 h at $T = 473$ K and atmospheric pressure before an uptake experiment of Cl_2 was carried out in the 14 mm-orifice reactor at $[Cl_2] = 2 \times 10^{11}$ molecule cm^{-3}. The γ_0 value remains unchanged but the Cl_2 uptake saturates faster than on a standard grain sample. The number of reactive sites able to take up Cl_2 decreases when the sample was previously heated. This is in agreement with the observation of a transition towards a better-ordered, hence more crystalline and therefore less-reactive surface. This crystallographic effect has been discussed before for thin KBr films sprayed on a gold-coated sample holder (Figs. 3a and 3c).

The fact that the initial uptake coefficient, γ_0, essentially remains unchanged upon heating suggests that the uptake kinetics of Cl_2 on a virgin KBr sample is determined by the geometrical extent or surface coverage of the SAW reservoir enabling the formation of the hydrated ion pairs and located between the two interfaces displayed in Fig. 10 rather than by the number of reactive surface sites located at the solid/SAW interface (zone 2, Fig. 10). From the foregoing it is expected that heating leads to crystallization of the bulk KBr/SAW interface (zone 2, Fig. 10) which would reduce the number of the available reaction sites. Loss of SAW by evaporation at ambient temperature through pumping, on the other hand, is expected to primarily affect the extent of the SAW reservoir and should leave the properties of the bulk KBr/SAW interface unchanged. However, prolonged pumping may also affect the surface coverage of SAW, hence the rate of uptake, such that the unambiguous separation of the heating effect and the SAW removal through pumping becomes uncertain.

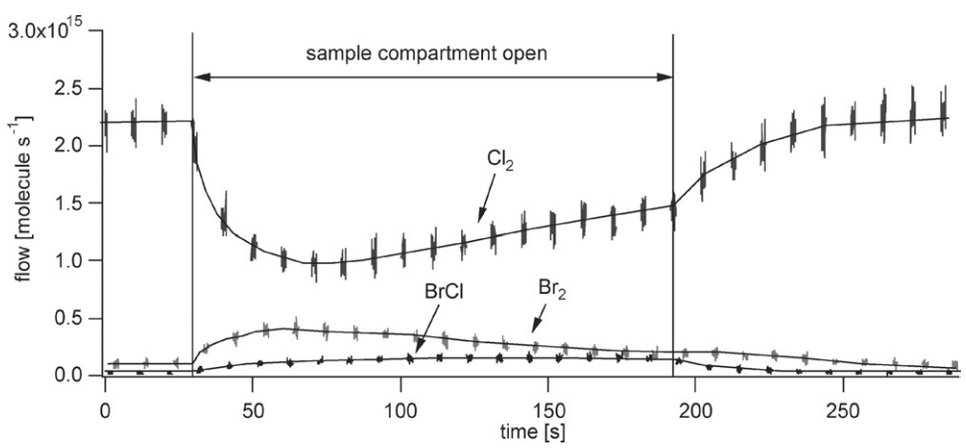

Fig. 11 Cl_2 uptake experiment carried out on KBr grains in the 1 mm-orifice reactor. Cl_2, Br_2 and BrCl are monitored at m/z 70, m/z 160 and m/z 116.

D. Cl_2O on NaCl substrates

Steady-state uptake experiments on NaCl and KBr grains have been carried out in the 4 and 14 mm-orifice reactor in order to provide a basis for comparison with HOCl whose anhydride is Cl_2O.[26] Additional experiments have been performed on KBr ground grains and thin KBr films sprayed on a Pyrex sample holder. The Cl_2O uptake experiments performed on the bare Pyrex sample-holder have not led to uptake of Cl_2O.

The Cl_2O uptake experiments performed on NaCl substrates lead to formation of Cl_2 and HOCl whereas on KBr substrates formation of Br_2, BrCl and slow formation of HOCl, HOBr and Cl_2 have been observed. Similar to uptake experiments of Cl_2 on solid KBr substrates steady-state experiments of Cl_2O on NaCl and KBr substrates have shown different behaviour between a fresh and an already exposed or poisoned sample. The differences were observed in relation to the uptake kinetics, as well as the formation of reaction products. This shows that for the reaction of Cl_2O on KBr and NaCl substrate, surface contamination also plays an important role. Details on the reaction of Cl_2O with solid KBr may be found in the Appendix.

In order to investigate the role of adsorbed reaction products multiple uptake experiments have been carried out on the same NaCl sample. Fig. 12 shows the formation of Cl_2 resulting from Cl_2O uptake experiments performed sequentially on NaCl grains in the 4 mm-orifice reactor. The first uptake experiment shows an induction time for the formation of Cl_2 after lifting the plunger, whereas further uptake experiments do not, and lead to the formation of Cl_2 at once after lifting the plunger. We suggest that this behaviour is related to the contamination of the surface due to the presence of surface-adsorbed halogen species. The short delay of Cl_2 formation in successive Cl_2O uptake experiments except the first are related to the filling of the reactor volume.

Uptake experiments of HOCl on solid KBr which will be discussed in a forthcoming paper[26] have shown that HOCl may adsorb on the KBr substrate. Similarly, we suggest that HOCl may adsorb on the surface of a solid NaCl substrate and may play a crucial role in the reaction with Cl_2O according to reaction (20).

$$Cl_2O(g) + SAW \rightarrow HOCl(g) + HOCl(a) \qquad (20)$$

In order to study the role of surface-adsorbed HOCl(a), as proposed in reaction (20) a series of Cl_2O uptake experiments have been carried out. The formation of HOCl and Cl_2 has been monitored and the total amount of lost Cl_2O and formed Cl_2 and HOCl has been determined. Fig. 13 shows the ratio R_1 of the yield of Cl_2 to lost Cl_2O, $R_1 = \frac{N_{Cl_2}}{\Delta N_{Cl_2O}}$, as well of the yield of HOCl and lost Cl_2O, $R_2 = \frac{N_{HOCl}}{\Delta N_{Cl_2O}}$, as a function of the number of uptake experiments or dose applied to the NaCl sample.

With the number of uptake experiments, n, performed on the same NaCl grain sample the amount of formed HOCl decreases in contrast to Cl_2. The ratio of the number of produced Cl_2, N_{Cl_2}, and the number of lost Cl_2O, N_{Cl_2O}, tends towards 2 with increasing n, $R_1 = \frac{N_{Cl_2}}{\Delta N_{Cl_2O}} \xrightarrow{n} 2$, whereas the ratio of produced HOCl to lost Cl_2O tends to a small value or zero $R_2 = \frac{N_{HOCl}}{\Delta N_{Cl_2O}} \xrightarrow{n} 0$. The fact that on a fresh NaCl sample the yield of HOCl corresponds to the loss of Cl_2O, as indicated by the first point in Fig. 13 leads us to the conclusion that Cl_2O reacts with SAW, as indicated by reaction (20) with one HOCl desorbing into the gas phase and hence detected, whereas one HOCl remains adsorbed on the substrate. Thus, adsorbed HOCl(a) contributes to contamination of the NaCl substrate. The yield of Cl_2 goes from zero for the uptake on a virgin sample to twice the amount of Cl_2O lost with increasing chlorine contamination of the surface.

This suggests that Cl_2O does not directly interact with the NaCl ion-pair but rather with SAW. For the interaction of HOCl with solid KBr we have proposed a screening of the KBr ion-pairs by SAW molecules as will be discussed in a forthcoming paper.[26] According to reaction (20) we may expect that formation of HOCl sets in immediately after the start of the reaction, whereas formation of Cl_2 is delayed as shown by the slow rise of Cl_2 formation displayed in Fig. 12. This suggestion is also supported by the fact that uptake experiments performed in the 14 mm-orifice reactor at very low Cl_2O concentration of 1×10^{10} molecule cm^{-3} only revealed the formation of HOCl, but no Cl_2.

The fact that HOCl has been observed immediately after lifting the plunger according to reaction (20) and that the formation of gaseous Cl_2 occurs with a delay implies that the chloride ion of the solid sample is not readily accessible to gaseous species and that the reaction starts with the initial interaction with SAW. Based on the fact that further uptake experiments of Cl_2O on a poisoned NaCl substrate lead to immediate formation of Cl_2 we propose that on a poisoned substrate Cl^- ions become directly available for gaseous reactants, such as in reaction (21).

$$Cl_2O(g) + Cl_{(surface)}{}^- \rightarrow ClO_{(surface)}{}^- + Cl_2(g) \qquad (21)$$

We suggest that the adsorption of HOCl on the NaCl substrate may reduce the proposed screening of the Na–Cl ion pair by SAW[26] and the chloride ion $Cl_{(surface)}{}^-$ becomes accessible for a reaction with gaseous $Cl_2O(g)$ as displayed in reaction (21). Above, we have suggested the dehydration of the surface by adsorbing halogen species according to reaction (14). We also propose that the dehydration of the surface may

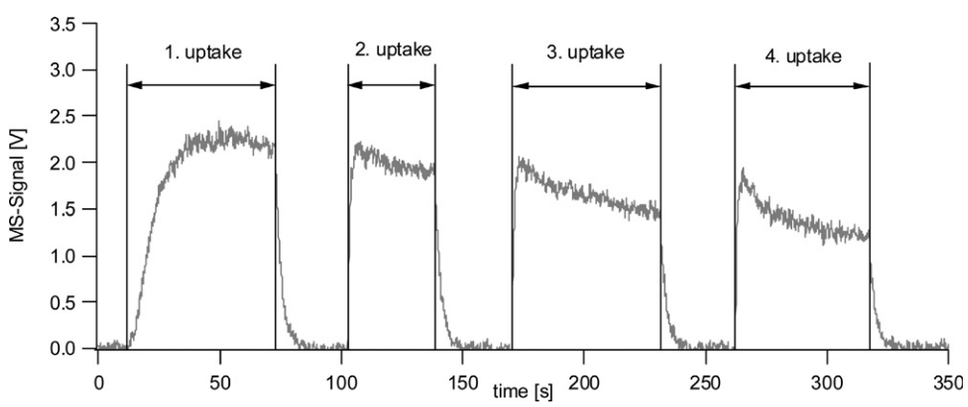

Fig. 12 MS-signal of the formation of Cl_2 in the reaction of Cl_2O on NaCl grains under steady-state conditions. The consecutive experiments have been carried out in the 4 mm-orifice reactor at $[Cl_2O] = 1 \times 10^{12}$ molecule cm^{-3}.

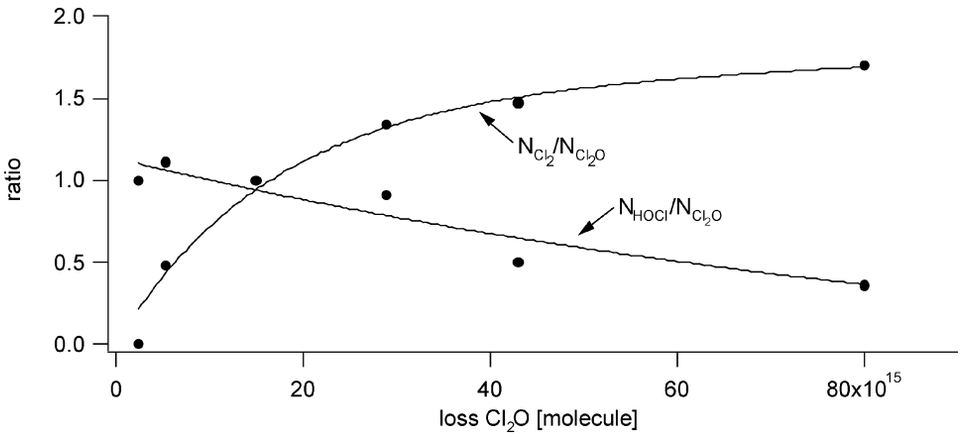

Fig. 13 Ratio between production of Cl_2 and HOCl and loss of Cl_2O, $R_1 = \frac{N_{Cl_2}}{\Delta N_{Cl_2O}}$ and $R_1 = \frac{N_{HOCl}}{\Delta N_{Cl_2O}}$, respectively, as a function of the amount of Cl_2O taken up by the same NaCl grain sample. The experiment has been carried out at Cl_2O concentrations between 1×10^{10} and 2×10^{12} molecule cm^{-3}.

weaken or counteract the screening of the hydrated Na–Cl ion-pair in order to enable the reaction between the "reactive" $Cl_{(surface)}^-$ and the gaseous reactant according to reaction (22). This process amounts to an activation of $Cl_{(surface)}^-$ for further reaction with gas phase and adsorbed species.

$$Na\text{–}Cl + ClO_{(surface)}^- \rightarrow Na^+ + Cl_{(surface)}^- + ClO(H_2O)_n(a) \quad (22)$$

Owing to the consumption of SAW more surface chloride is available for reaction according to reaction (21). This and the accumulation of HOCl(a) on the surface may explain the formation of up to two moles of Cl_2 per mole of Cl_2O lost on a poisoned substrate, according to Fig. 13 for large n and justifies the reaction scheme proposed below. For the reaction of Cl_2O on a fresh NaCl sample the mechanism starts with reaction (20) and the equilibrium of SAW with NaCl,[40] reaction (23):

$$NaCl(s) + SAW \rightleftarrows Na\text{–}Cl \quad (23)$$

$$Cl_2O(g) + SAW \rightleftarrows HOCl(a) + HOCl(g) \quad (20)$$

$$HOCl(a) + Na\text{–}Cl \rightarrow Cl_2(g) + NaOH(s) \quad (24)$$

$$\text{Net}: \quad Cl_2O(g) + NaCl(s) + SAW \rightarrow Cl_2(g) + HOCl(g) + NaOH(s)$$

This explains the immediate release of HOCl after lifting the plunger as well as the surface contamination by adsorbed HOCl. The induction time for the formation of Cl_2 is due to the slow secondary reaction of HOCl(a) with Na–Cl, reaction (24).

In order to explain the reaction on a poisoned NaCl substrate the following mechanism has been constructed:

$$NaCl(s) + SAW \rightleftarrows Na\text{–}Cl \quad (23)$$

$$Cl_2O(g) + Cl_{(surface)}^- \rightarrow Cl_2(g) + ClO_{(surface)}^- \quad (21)$$

$$ClO_{(surface)}^- + SAW \rightarrow HOCl(a) + OH_{(surface)}^- \quad (25)$$

$$HOCl(a) + Na\text{–}Cl \rightarrow Cl_2(g) + Na\text{–}OH \quad (24)$$

$$\text{Net}: \quad Cl_2O(g) + NaCl(s) + Cl_{(surface)}^- + SAW \rightarrow 2Cl_2(g) + NaOH(s) + OH_{(surface)}^-$$

The Cl^- ion involved in reaction (21) may be formed by dehydration of the surface, as discussed above (reaction (22)). The reaction of Cl_2O with solid NaCl clearly shows the importance of SAW and adsorbed halogens for the heterogeneous reactions of halogen species with alkali–halide substrates.

Conclusions

SAW

We found by using SEM-imaging that upon pumping, thin KBr films sprayed on a gold-coated copper support undergo a substantial change towards a higher degree of crystallinity due to dehydration of KBr. This is consistent with the presence of mobile ions on the KBr surface whose abundance is controlled by the amount of SAW. The observed crystallisation turns out to be irreversible. A change of the morphology upon heating of thin films of KBr to $T = 620$ K at 10^{-6} Torr background pressure of H_2O was also observed. This temperature is well below the melting point of KBr and implies that ionic diffusion processes apparently set in well below the melting point of KBr.

Upon heating of KBr ground grains and thin KBr films sprayed on a gold-coated copper sample holder to $T = 620$ K under vacuum conditions, desorption of HBr and HOBr has been observed whereas none could be detected for KBr grains. Mechanical stress such as grinding and rapid evaporation of the solvent of the salt solution may lead to a change in the oxidation state of bromine and, consequently, to a possible formation of surface adsorbed Br–Br pairs together with localised electrons trapped in F-centers or other lattice imperfections. HOBr and HBr is the result of the reverse disproportionation of Br_2(a) with SAW, reaction (8).

The presence of surface-bound basic sites or surface hydroxyl groups has been demonstrated by the interaction of the substrate with carbon dioxide, reaction (10). We estimated the number of basic sites to be less than 1% of the total number of surface sites.

The presence of mobile halogen ions on the surface leads to recrystallisation of a thin KBr film induced by the interaction of Br_2 with the KBr substrate. The presence of adsorbed Br_2(a) seems to lower the energy barrier for the transition from a low- to a higher-ordered crystalline state. The SAW on the surface of KBr enables the interaction with additional molecular halogens or interhalogens from the gas phase in order to establish equilibrium (6a). In agreement with this, a surface-residence time τ_s of Br_2 on standard KBr grains of 5 ms at 300 K has been measured.

Cl_2/KBr

Uptake experiments of Cl_2 on different KBr substrates have resulted mainly in the formation of Br_2 together with small amounts of BrCl. Under low-pressure conditions a slow partial regeneration of the sample has been observed as far as γ_0 is

concerned. This regeneration may be due to conversion of adsorbed chlorine to KCl accompanied by the formation of adsorbed polyhalide ions of the type Cl_2Br^- or Br_2Cl^- originating from KBr, reactions (16) and (17) which may build up reactive sites for further Cl_2 reaction.

Molecular chlorine and bromine may thus be retained on the surface and play a crucial role in terms of product yield and reaction kinetics. Exposure of a poisoned sample to ambient conditions essentially does not affect the initial reaction kinetics (γ_0) whereas the yield of Br_2 increases, following exposure to water vapor. In contrast to the heat treatment the prolonged evacuation of the KBr sample causes a considerable decrease in γ_0 by removing the weakly bound H_2O. The results are consistent with a double interface model that contains SAW leading to hydrated ion-pairs. Heating at ambient conditions leads to a recrystallization process at the bulk KBr/SAW interface (zone 2, Fig. 10) and therefore leads to reduction of the number of the active surface sites but leaves the volume of SAW unchanged. Pumping, on the other hand, modifies the volume of SAW and its coverage to a larger degree thereby affecting the properties of the gas/SAW interface (zone 1, Fig. 10) and will lead to a decrease of γ_0.

Cl_2O/NaCl

Uptake of Cl_2O on solid NaCl has led exclusively to HOCl at low, and to Cl_2 + HOCl at high partial pressure of Cl_2O in a reaction whose mass balance has shown a one to one correspondence between the loss of Cl_2O and the formation of HOCl (Fig. 13). This leads to the accumulation of chlorine species such as HOCl(a) on the NaCl surface. On a poisoned NaCl surface, the ratio R between Cl_2O lost and Cl_2 formed tends towards two with increasing Cl_2 dose (Fig. 13). The release of gaseous Cl_2 is delayed when an experiment on a fresh substrate is carried out whereas on a poisoned NaCl sample the uptake of Cl_2O leads to immediate formation of Cl_2. We propose the existence of a screening effect of SAW on the surface-ions (Fig. 10) that leads to a delay in the rate of Cl_2 formation and an increase in the Cl_2 yield upon repetitive exposure of NaCl to Cl_2O. The reaction of Cl_2O on different KBr substrates mainly led to formation of Br_2 and BrCl. In addition, slow production of HOCl, BrOCl and Cl_2 have also been detected.

We have shown in this work that for the reactions of halogen species with alkali salt substrates the contamination of the surface by adsorption of halogen species crucially influences the uptake kinetics. We conclude that under vacuum conditions, adsorbed halogen species may effectively dehydrate the alkali salt surface owing to competition for limited amounts of SAW. In this way, the screening of the ions may be weakened which activates the reactant ions and may increase their reactivity. Under ambient conditions corresponding to several Torr of H_2O vapor no activation is expected to take place because of unlimited availability of water vapor. The presence of H_2O may, on the other hand, lead to a higher mobility of the adsorbed halogens on the surface that may ultimately lead to higher yields of reaction products. This will have to be probed in experiments at high relative humidity.

Appendix. Uptake of Cl_2O on KBr substrates

The observed main reaction products of the reaction of Cl_2O with KBr are Br_2 and BrCl. Furthermore, slow production of HOCl, BrOCl and Cl_2 have also been detected. In order to check the sample for adsorbed Cl_2O stopped-flow experiments have been carried out similar to the ones already performed on Br_2 on KBr substrates (see main text). In contrast to the Br_2 experiments the decay rate of the Cl_2O MS-signal in the presence of the KBr substrate is identical to the decay in the absence of the sample. This means that, in contrast to Cl_2 and Br_2, Cl_2O does not significantly stick to the surface of the KBr sample but undergoes a prompt reaction on the substrate. No surface residence time τ could therefore be measured for Cl_2O interacting with solid KBr.

In order to investigate the role of surface contamination subsequent uptake experiments have been carried out on the same substrate. Fig. 14 shows the rate of formation of Br_2 in subsequent uptake experiments performed on the same KBr grain sample. With the number of Cl_2O uptake experiments Br_2 shows a more pronounced peak in the rate of formation after lifting the plunger, but saturates faster. Similar behaviour, albeit less pronounced, has been observed for the BrCl production rate. The mass balance according to overall reactions (A1) and (A2) results in a deficit of reaction products which may be explained by adsorption of bromine, as we have already discussed above.

$$Cl_2O(g) + 2KBr(s) \rightarrow Br_2(g) + \text{adsorbed products} \quad (A1)$$

$$Cl_2O(g) + KBr(s) \rightarrow BrCl(g) + \text{adsorbed products} \quad (A2)$$

The reaction of Cl_2O with SAW, reaction (20), plays a crucial role both on solid NaCl as well as on KBr. In contrast to the reaction of Cl_2O with NaCl, the reaction of Cl_2O with KBr leads to slow formation of HOCl and Cl_2 only on a poisoned KBr sample. Similar to reaction (22) we propose the following reaction:

$$K\text{–}Br + ClO_{(surface)}^- \rightarrow K^+ + Br_{(surface)}^- + ClO^-(H_2O)_n(a) \quad (A3)$$

where adsorbed ClO^- may be formed by hydration of HOCl(a):

$$HOCl(a) + SAW \rightarrow H^+ + ClO_{(surface)}^- \quad (A4)$$

The adsorbed ClO^- binds SAW and a lack of SAW therefore arises. The Br^- ion is activated in reaction (A3) and is therefore easily available for surface reactions. This leads to the following reaction mechanism:

$$2\ (KBr(s) + SAW \rightleftarrows K\text{–}Br) \quad (A5)$$

$$Cl_2O(g) + SAW \rightleftarrows HOCl(a) + HOCl(g) \quad (20)$$

$$HOCl(a) + SAW \rightarrow H^+ + ClO_{(surface)}^- \quad (A4)$$

$$K\text{–}Br + ClO_{(surface)}^- \rightarrow K^+ + Br_{(surface)}^- + ClO^-(H_2O)_n(a) \quad (A3)$$

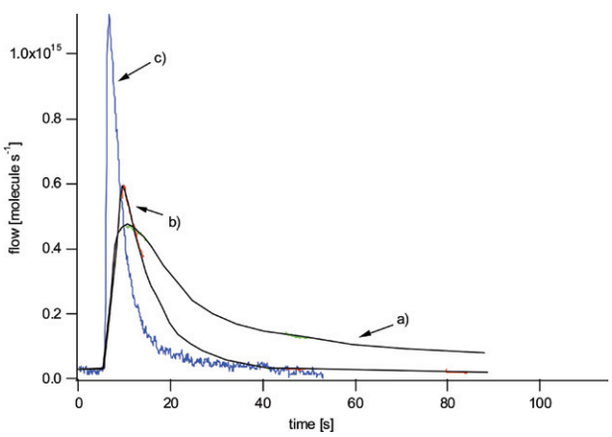

Fig. 14 Br_2 rate of formation resulting from steady-state Cl_2O uptake experiment on KBr grains carried out in the 4 mm-orifice reactor. The graphs display the rate of production of Br_2 in subsequent uptake experiments: (a) first uptake, (b) second uptake, and (c) sixth uptake experiment, all using the same Cl_2O dose.

$$HOCl(g) + K^+ + Br_{(surface)}{}^- \rightarrow BrCl(a) + K^+ + OH_{(surface)}{}^- \quad (A6)$$

$$BrCl(a) + K{-}Br \rightarrow K{-}Cl + Br_2(g) \quad (A7)$$

$$H^+ + K^+ + OH_{(surface)}{}^- \rightarrow K^+ + SAW \quad (A8)$$

$$K^+ + ClO^-(H_2O)_n(a) \rightarrow K{-}OCl \quad (A9)$$

$$\text{Net}: \quad Cl_2O(g) + 2KBr + 3SAW \rightarrow K{-}Cl + K{-}OCl + Br_2(g)$$

Adsorption of chlorine-containing species drives the bromide of the substrate towards the surface according to reaction (A3) where it becomes available for reaction with gaseous species.

The formation of HOCl, Cl_2 and HOBr on a poisoned sample may be explained by the accumulation of KOCl on the surface followed by fast hydrolysis, reaction (A10) and the reaction of BrCl(a) with adsorbed HOCl(a), reaction (A11), respectively.

$$KOCl(s) + SAW \rightleftarrows KOH + HOCl(g) \quad (A10)$$

$$HOCl(a) + BrCl(a) \rightarrow Cl_2(g) + HOBr(g) \quad (A11)$$

In this section we have demonstrated that adsorbed halogen species and SAW also play a crucial role for the reaction of Cl_2O on KBr substrates. In analogy to the reaction of Cl_2O on NaCl we propose that no direct reaction of Cl_2O with KBr takes place. Cl_2O interacts first with the SAW and the adsorbed HOCl(a) may undergo consecutive reactions in order to form gaseous $Br_2(g)$ such as in reactions (A6) and (A7). The mass balance points to a deficiency in Br_2 compared to the loss of Cl_2O akin to Cl_2O/NaCl. This led to the conclusion of the existence of adsorbed ionic polyhalogen species on solid KBr. Repetitive uptake experiments showed that Br_2 is formed more rapidly on an already poisoned KBr sample. The primary product HOCl(a) effectively competes for SAW that was previously bound to KBr, as represented in reaction (A4). This adsorption thus activates Br^- for reaction with gas and adsorbed molecules in analogy to the activation mechanism for solid NaCl.

Acknowledgements

We are grateful for generous funding of this project by Office Fédéral de l'enseignement et de la science (OFES). It was carried out in the 5th framework program of the EU Environment and Climate program within the subproject HAMLET.

References

1 G. A. Impey, P. B. Shepson, D. R. Hastie, L. A. Barrie and K. G. Anlauf, *J. Geophys. Res. Atmos.*, 1997, **102**, 16 005–16 010.
2 U. Langendorfer, E. Lehrer, D. Wagenbach and U. Platt, *J. Atmos. Chem.*, 1999, **34**, 39–54.
3 U. Platt, *Water Air Soil Pollut.*, 2000, **123**, 229–244.
4 U. Platt and M. Hausmann, *Res. Chem. Intermed.*, 1994, **20**, 557–578.
5 B. J. Finlayson-Pitts, *Res. Chem. Intermed.*, 1993, **19**, 235–249.
6 B. J. Finlayson-Pitts, F. E. Livingston and H. N. Berko, *Nature (London)*, 1990, **343**, 622–625.
7 L. A. Barrie, J. W. Bottenheim, R. C. Schnell, P. J. Crutzen and R. A. Rasmussen, *Nature (London)*, 1988, **334**, 138–141.
8 C. W. Spicer, E. G. Chapman, B. J. Finlayson-Pitts, R. A. Plastridge, J. M. Hubbe, J. D. Fast and C. M. Berkowitz, *Nature (London)*, 1998, **394**, 353–356.
9 J. H. Seinfeld and S. N. Pandis, *Atmospheric Chemistry and Physics*, John Wiley & Sons, New York, 1998.
10 U. Platt and G. K. Moortgat, *J. Atmos. Chem.*, 1999, **34**, 1–8.
11 A. A. P. Pszenny, W. C. Keene, D. J. Jacob, S. Fan, J. R. Maben, M. P. Zetwo, M. Springeryoung and J. N. Galloway, *Geophys. Res. Lett.*, 1993, **20**, 699–702.
12 P. V. Hobbs, *Introduction to Atmospheric Chemistry*, Cambridge University Press, Cambridge, 2000.
13 D. O. De Haan, T. Brauers, K. Oum, J. Stutz, T. Nordmeyer and B. J. Finlayson-Pitts, *Int. Rev. Phys. Chem.*, 1999, **18**, 343–385.
14 P. Wennberg, *Nature (London)*, 1999, **397**, 299–301.
15 M. Hausmann and U. Platt, *J. Geophys.Res. Atmos.*, 1994, **99**, 25 399–25 413.
16 L. Barrie and U. Platt, *Tellus Ser. B*, 1997, **49**, 450–454.
17 C. T. McElroy, C. A. McLinden and J. C. McConnell, *Nature (London)*, 1999, **397**, 338–341.
18 H. C. Allen, J. M. Laux, R. Vogt, B. J. Finlayson-Pitts and J. C. Hemminger, *J. Phys. Chem.*, 1996, **100**, 6371–6375.
19 P. Beichert and B. J. Finlayson-Pitts, *J. Phys. Chem.*, 1996, **100**, 15 218–15 228.
20 J. A. Davies and R. A. Cox, *J. Phys. Chem. A*, 1998, **102**, 7631–7642.
21 S. Ghosal and J. C. Hemminger, *J. Phys. Chem. A*, 1999, **103**, 4777–4781.
22 J. M. Laux, J. C. Hemminger and B. J. Finlayson Pitts, *Geophys. Res. Lett.*, 1994, **21**, 1623–1626.
23 Q. Dai, J. Hu and M. Salmeron, *J. Phys. Chem. B*, 1997, **101**, 1994–1998.
24 B. Wassermann, S. Mirbt, J. Reif, J. C. Zink and E. Matthias, *J. Chem. Phys.*, 1993, **98**, 10 049–10 060.
25 S. Fölsch, A. Stock and M. Henzler, *Surf. Sci.*, 1992, **264**, 65–72.
26 C. Santschi and M. J. Rossi, in preparation.
27 F. Caloz, F. F. Fenter, K. D. Tabor and M. J. Rossi, *Rev. Sci. Instrum.*, 1997, **68**, 3172–3179.
28 F. Caloz, EPFL, 1997.
29 H. D. Knauth, H. Alberti and H. Clausen, *J. Phys. Chem.*, 1979, **83**, 1604–1612.
30 R. C. Weast, *Handbook of Chemistry and Physics*, CRC Press, New York, 67th edn., 1986.
31 L. F. Keyser, S. B. Moore and M. T. Leu, *J. Phys. Chem.*, 1991, **95**, 5496–5502.
32 C. Santschi, PhD Thesis, Swiss Federal Institute of Technology, EPFL, 2003.
33 H. U. Walter, *Z. Phys. Chem. (Frankfurt)*, 1971, **75**, 287–298.
34 L. Gutzwiller, PhD Thesis, Ecole Polytechnique Fédérale de Lausanne (EPFL), 1996.
35 M. F. Butman, A. A. Smirnov, L. S. Kudin and Z. A. Munir, *J. Mater. Synth. Process.*, 2000, **8**, 55–63.
36 M. F. Butman, A. A. Smirnov, L. S. Kudin and Z. A. Munir, *Surf. Sci.*, 2000, **458**, 106–112.
37 L. G. Harrison, J. A. Morrison and G. S. Rose, *J. Phys. Chem.*, 1957, **61**, 1314–1318.
38 L. G. Harrison, J. A. Morrison and R. Rudham, *Trans. Faraday Soc.*, 1958, **54**, 106–115.
39 I. N. Tang and K. H. Fung, *J. Chem. Phys.*, 1997, **106**, 1653–1660.
40 D. J. Dai, S. J. Peters and G. E. Ewing, *J. Phys. Chem.*, 1995, **99**, 10 299–10 304.
41 C. Kittel, *Einführung in die Festkörperphysik*, ed. R. Oldenbourg, Verlag, 10th edn., 1993.
42 J. K. S. Wan, J. N. Pitts, P. Beichert and B. J. FinlaysonPitts, *Atmos. Environ.*, 1996, **30**, 3109–3113.
43 D. A. Otterson, *J. Chem. Phys.*, 1963, **38**, 1481–1486.
44 A. Aguzzi and M. J. Rossi, *Phys. Chem. Chem. Phys.*, 1999, **1**, 4337–4346.
45 D. D. Wagman, W. H. Evans, V. B. Parker, R. H. Schumm, I. Halow, S. M. Bailey, K. L. Churney and R. L. Nuttal, *The NBS Tables of Chemical Thermodynamic Properties*, American Chemical Society, 1982, vol. 11.
46 B. J. Finlayson-Pitts and J. C. Hemminger, *J. Phys. Chem. A*, 2000, **104**, 11 463–11 477.
47 J. M. Laux, T. F. Fister, B. J. FinlaysonPitts and J. C. Hemminger, *J. Phys. Chem.*, 1996, **100**, 19 891–19 897.
48 L. Degreve and F. L. B. da Silva, *J. Chem. Phys.*, 1999, **111**, 5150–5156.
49 C. D. Zangmeister and J. E. Pemberton, *J. Phys. Chem. A*, 2001, **105**, 3788–3795.
50 M. Mochida, J. Hirokawa, Y. Kajii and H. Akimoto, *Geophys. Res. Lett.*, 1998, **25**, 3927–3930.
51 A. K. Galwey and L. Poppl, *Nature (London)*, 1981, **294**, 434–436.
52 J. W. Adams, N. S. Holmes and J. N. Crowley, *Atmos. Chem. Phys.*, 2002, **2**, 79–91.
53 F. F. Fenter, F. Caloz and M. J. Rossi, *J. Phys. Chem.*, 1994, **98**, 9801–9810.
54 H. N. Berko, P. C. McCaslin and B. J. Finlayson-Pitts, *J. Phys. Chem.*, 1991, **95**, 6951–6958.
55 T. E. Graedel and W. C. Keene, *Global Biogeochem. Cycles*, 1995, **9**, 47–77.
56 NIST-Chemistry-WEBBook (http://webbook.nist.gov/chemistry/).

